

Reconfigurable Intelligent Surface: Power Consumption Modeling and Practical Measurement Validation

Jinghe Wang, Wankai Tang, Jing Cheng Liang, Lei Zhang, Jun Yan Dai,
Xiao Li, Shi Jin, Qiang Cheng, and Tie Jun Cui

Abstract—Due to the ability to reshape the wireless communication environment in a cost- and energy-efficient manner, the reconfigurable intelligent surface (RIS) has garnered substantial attention. However, the explicit power consumption model of RIS and measurement validation, have received far too little attention. Therefore, in this work, we propose the RIS power consumption model and implement the practical measurement validation with various RISs. Measurement results illustrate the generality and accuracy of the proposed model. Firstly, we verify that RIS has static power consumption, and present the experiment results. Secondly, we confirm that the dynamic power consumption of the varactor-diode based RIS is almost negligible. Finally but significantly, we model the quantitative relationship between the dynamic power consumption of the PIN-diode based RIS and the polarization mode, controllable bit resolution, working status of RIS, which is validated by practical experimental results.

Index Terms—Reconfigurable intelligent surface (RIS), power consumption model, measurement validation

I. INTRODUCTION

FUTURE wireless communication systems will need to meet a wide range of extremely-high requirements, which drives the sixth generation (6G) dedicated to introducing a variety of developing technologies. The reconfigurable intelligent surface (RIS), a prospective 6G technology, has recently gained the attention of the wireless research community. RIS consists of arranged artificial two-dimensional electromagnetic unit cells and hardware control circuits. Unit cells are typically made of metals, media, and adjustable components (i.e., varactor diodes and PIN diodes), which can regulate and control the space electromagnetic waves by adjusting the electromagnetic parameters such as the phase, amplitude, and polarization [1]. When there is no direct link between the base station (BS) and the user equipment (UE), RIS can be deployed to provide additional virtual line-of-sight (vLoS) links for signal transmission. The beam reflected by RIS can be tailored to a particular transmission by modifying the phase, so as to lower the transmission power, increase spectrum

efficiency, and broaden the coverage of the system. System performance enhancement can be achieved through the joint active beamforming at the BS and passive beamforming (phase shift design) at the RIS [2]-[3]. Particularly, the lower power consumption of RIS is a major draw. However, the explicit power consumption modeling of RIS and the model validation have received far too little research up to this point.

In the following work, we focus on the power consumption research of RIS. Up to now, limited research has investigated on this topic. In [4], the authors developed a total power consumption model of the RIS-based system, which helps formulate and solve the energy efficiency (EE) maximization problem for the joint active and passive beamforming design. Based on the power consumption of the conventional phase shifter in RF circuits [5], the authors in [4] claim that the RIS power consumption depends on the number of RIS unit cells and the resolution of its individual unit cell. And the power consumption of RIS is modeled as $P_{\text{RIS}} = NP_n(b)$, where N is the number of identical RIS unit cells and $P_n(b)$ denotes the power consumption of each RIS unit cell having b -bit resolution. However, both the power consumption of the control circuit and the effect of unit cell coding on power consumption are not considered. Moreover, the specific relationship between b and power consumption is not clearly given. In [6], the authors develop a total power consumption model, where the process and the power consumption of the channel state information (CSI) estimation and feedback are additionally considered compared with [4]. Nevertheless, this work still mainly focuses on solving the optimization problems for the phase shift design of RIS, system transmission and reception, channel estimation and feedback, and did not illustrate the power consumption model of RIS in depth. Specific measurements of RIS power consumption are mentioned in [7]-[8]. The authors in [7] illustrate some preliminary measurement results of RIS power consumption, which show that different kinds of RIS have different power consumption characteristics. However, it has not been further modeled and discussed. In [8], a detailed description of the power consumption of the fabricated varactor-diode based RIS is shown, which claims that this kind of RIS consumes little power, showing the great potential of RIS for future communication systems. So far, little research of the power consumption modeling and practical measurement validation has been reported to date. This thus motivates this work to fill this vacancy. In the following work, we report the first general RIS power consumption model and

Jinghe Wang, Wankai Tang, Xiao Li and Shi Jin are with the National Mobile Communications Research Laboratory, Southeast University, Nanjing 210096, China (e-mail: wangjh@seu.edu.cn; tangwk@seu.edu.cn; li_xiao@seu.edu.cn; jinshi@seu.edu.cn).

Jing Cheng Liang, Lei Zhang, Jun Yan Dai, Qiang Cheng, and Tie Jun Cui are with the State Key Laboratory of Millimeter Waves, Southeast University, Nanjing 210096, China (e-mail: jingcheng_liang@foxmail.com; cheunglee@126.com; junyand@seu.edu.cn; qiangcheng@seu.edu.cn; tjcui@seu.edu.cn).

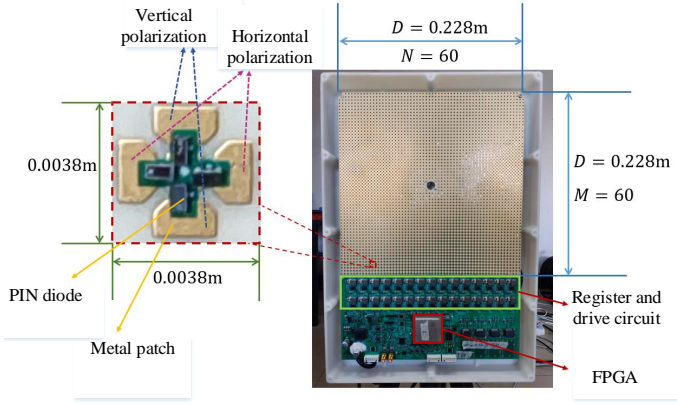


Fig. 1: Photograph of the 1st dual-polarized PIN-diode based RIS.

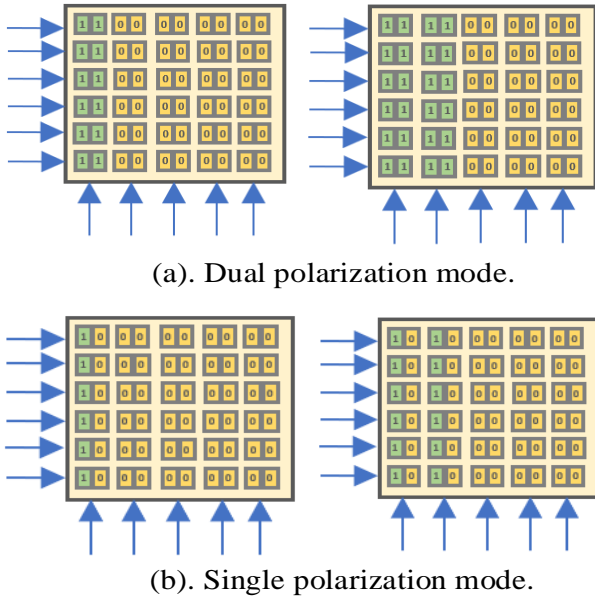


Fig. 2: Enabling the 1st RIS by column. (a) Dual polarization mode. (b) Single polarization mode.

practical power consumption measurements are implemented for validation. The establishment of a practical RIS power consumption model helps accurately characterize the system power consumption and energy efficiency performance of the RIS-assisted wireless communication system, which provides a significant basis for subsequent wireless system optimization design and algorithm performance evaluation.

II. PRELIMINARY POWER CONSUMPTION MODELING

The total power dissipated to operate the RIS is composed of two parts, one is the static power consumption generated by the control circuit (i.e., PIN diodes with FPGAs and registers, varactor diodes with digital to analog converters (DACs) or voltage level shifter circuitry), the other is the dynamic power consumption generated by the RIS unit cells [7]. Accordingly, the total power consumption modeling of RIS can be expressed as follows:

$$P_{\text{RIS}} = P_{\text{static}} + P_{\text{dynamic}} \quad (1)$$

TABLE I: Indicator Parameters of Polarization Mode

	I_v	I_h
Dual polarization	1	1
Horizontal polarization	0	1
Vertical polarization	1	0

where P_{static} is the static power consumption and P_{dynamic} is the dynamic power consumption.

For the RIS belonging to the family of varactor-diode-based programmable metasurfaces, the dynamic power consumption is regarded as 0, since the current in the varactor diodes of the unit cells is negligible when it is working, even though the unit cells are large in number, which are supported by practical measurements [7]-[8].

As for the PIN-diode-based RIS, the dynamic power consumption needs to be considered more thoughtfully. Firstly, the dynamic power consumption is affected by polarization mode. More PIN diodes need to be embedded on dual polarization RIS to achieve polarization in both directions at the same time, which will affect the power consumption. Secondly, the dynamic power consumption is affected by bit resolution of RIS unit cells. Two working states of a single PIN diode can be represented by 1-bit binary state, while a multi-bit unit cell need to be realized by multiple PIN diodes, which will affect the power consumption. Thirdly, the dynamic power consumption is affected by unit cell coding status. For example, a 2-bit RIS unit cell has 4 coding statuses, which can be denoted as “00”, “01”, “10”, and “11”. The number of “on-state” PIN diodes is different in 4 coding states, thus the power consumption is also different. Accordingly, P_{dynamic} can be expressed as (2) in the next page.

Specifically in (2), I_v , I_h denote the indicator parameters of vertical polarization and horizontal polarization respectively, and the parameter “1” indicates that RIS can control incident wireless signals in this polarization direction. The indicator parameters of polarization mode is shown in Table I. N is the number of RIS unit cells. $P_{i,x}(B_{i,x}, b_{i,x})$ ($x = v, h$) is the power consumption of the i -th RIS unit cell with B -bit resolution in single polarization mode, which can be denoted as

$$P_{i,x}(B_{i,x}, b_{i,x}) = b_{i,x} \cdot P_{\text{PIN}}, 0 \leq b_{i,x} \leq B_{i,x} \quad (3)$$

where $B_{i,x}$ is the bit resolution of RIS unit cell, $b_{i,x}$ is the number of bit encoded as “1”, and P_{PIN} is power consumption of PIN diodes for supporting one bit encoded as “1”. It is worth noting that all unit cells of a RIS are set to the same bit resolution for simpler hardware design, thus $B_{i,x}$ in (3) can be reduced to B_x . The formula (3) shows that the power consumption of each unit cell not only depend on the inherent quantization bit B of the unit, but also on the coding state of the unit. For each bit of the unit cell, the power is consumed only when encoded as “1”, and the power consumption is 0 when encoded as “0”.

III. PRACTICAL MEASUREMENT AND VALIDATION

Experimental measurements are carried out to validate the proposed preliminary power consumption model for RIS. Three PIN-diode-based RIS and one varactor-diode-based RIS are utilized for validation, respectively.

$$P_{\text{dynamic}} = \begin{cases} I_v \cdot \sum_{i=1}^N [P_{i,v}(B_{i,v}, b_{i,v})] + I_h \cdot \sum_{i=1}^N [P_{i,h}(B_{i,h}, b_{i,h})], & \text{PIN-diode-based RIS} \\ 0, & \text{varactor-diode-based RIS} \end{cases} \quad (2)$$

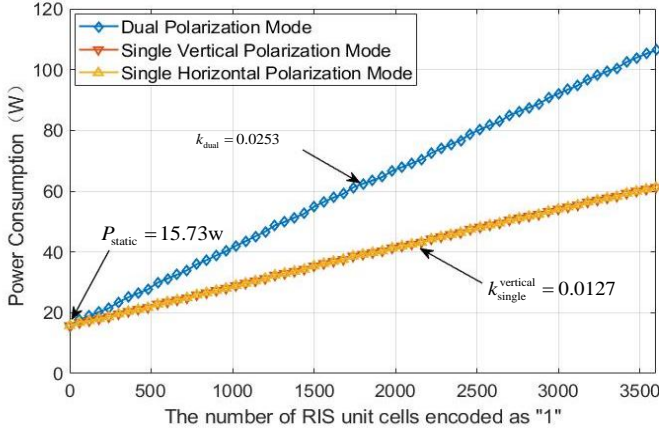


Fig. 3: The total power consumption v.s. The number of RIS unit cells encoded as “1”.

A. PIN-diode-based RIS

1) *1[#] RIS*: The fabricated RIS utilized for first verification belongs to the family of PIN-diode-based programmable metasurfaces, which is phase-programmable with 1-bit coding, as shown in Fig. 1. It is a dual-polarized RIS, which can control the phase shift of reflected EM waves in two polarizations and the operating frequency is $f = 35$ GHz. The total length and width of the dual-polarized RIS are $0.228 \text{ m} \times 0.228 \text{ m}$, and the RIS is composed of 60×60 reduplicated unit cells, with each unit cell having a length and width of $38 \text{ mm} \times 38 \text{ mm}$ and being regulated independently. The unit cell consists of the substrate, two pairs of mutually perpendicular metal patches, and two pairs of PIN diodes connected across the metal patches. For each unit cell, two bias voltages are applied to the two pairs of PIN diodes through metal patches. The bias voltages can change the reflection coefficient of the unit cell for vertical polarization and horizontal polarization.

In the following power consumption measurement, a 0 V voltage is applied to achieve the “0” coding status, and a high (i.e., higher than conductive voltage of PIN diodes) voltage is applied to achieve the “1” coding status of RIS unit cell. Firstly, all PIN diodes are encoded as “0”, and all PIN diodes are “off-state” because 0 V voltage does not achieve the conductive voltage of PIN diodes. Therefore, the power consumption at this time is mainly the static power consumption of the control circuit (mainly included FPGA and shift register), measured as 15.75 W. Secondly, all PIN diodes are encoded as “1”. In this case, all PIN diodes are “on-state” and consume energy, and the maximum power consumption of the PIN-diode-based RIS is measured as 103.2 W. Next, starting from the “0” coding status, each column of the RIS unit cells are switched from “0” to “1”, as shown in Fig. 2. The power consumption of each measurement are recorded accordingly.

We fit the data of enabling the RIS by column, as shown in Fig. 3. At first, we observe that there exists a linear relationship

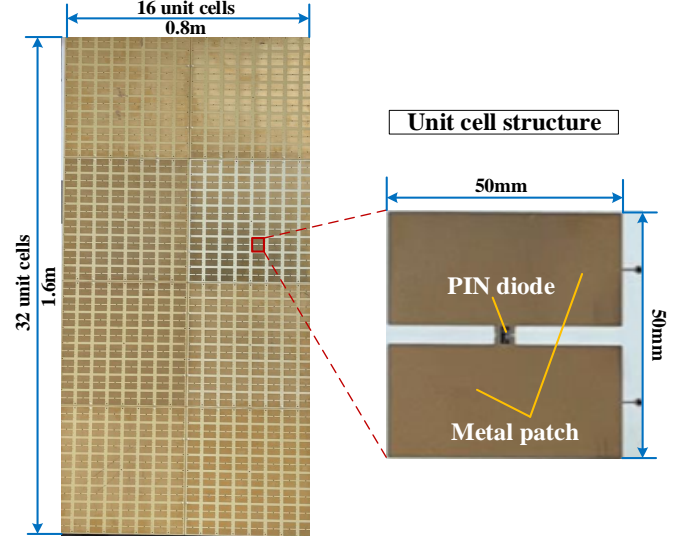


Fig. 4: Photographs of the 2[#] fabricated PIN-diode-based RIS wall.

between the total power consumption of RIS and the number of RIS unit cells encoded as “1” (denoted as n). When $n = 0$, $P_{\text{static}} = 15.73 \text{ W}$, which is the static power consumption; With the increment of n , the total power consumption of RIS increases. When n is the same, the power consumption of single vertical/horizontal polarization are approximately equal, and the curves are nearly coincident. Moreover, it can be seen that the power consumption of dual polarization mode is twice as much as that in single polarization mode, denoted as $k_{\text{dual}} \approx 2k_{\text{single}}^{\text{vertical}} \approx 2k_{\text{single}}^{\text{horizontal}}$. Therefore, the practical power consumption measurement of 1[#] RIS is consistent with the proposed model in (2). According to the measurement results, the key parameters of 1[#] RIS in the model are: $P_{\text{static}} = 15.73 \text{ W}$, $P_{i,v}(1, 0) = P_{i,h}(1, 0) = 0$, and $P_{i,v}(1, 1) = P_{i,h}(1, 1) = P_{\text{PIN}} = 12.56 \text{ mW}$, $1 \leq i \leq 3600$.

2) *2[#] RIS*: Another PIN-diode-based RIS utilized for a second measurement is also a 1-bit coding phase-programmable metasurface, operating at $f = 2.6$ GHz, as shown in Fig. 4. The total length and width of this RIS are $1.6 \text{ m} \times 0.8 \text{ m}$, and the RIS is composed of 32×16 reduplicated unit cells, with each unit cell having a length and width of $50 \text{ mm} \times 50 \text{ mm}$ and being regulated independently. The overall power consumption of the RIS is 12.66 W when all unit cells are encoded as “1” and 6.52 W when all unit cells are encoded as “0”.

This RIS is also encoded from “0” to “1” by column control from left to the right and the power consumption are measured and recorded accordingly. The linear relationship between the total power consumption of RIS and the number of RIS unit cells encoded as “1” (denoted as n) resemble the first fabricated RIS measurement. When $n = 0$, $P_{\text{static}} = 6.52 \text{ W}$, which is the static power consumption; With the increment of n , the total power consumption of RIS increases. Moreover, a random encoding measurement is carried for another model validation.

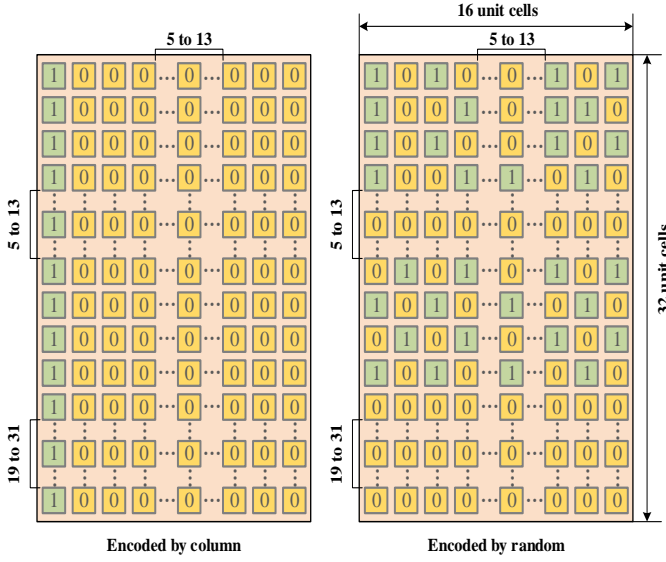


Fig. 5: Enabling the RIS by column and random.

Rather than encoding the RIS by column, the RIS is enabled by random. Encoding the random 32 unit cells as “1” consumes the same power compared with encoding the first column of RIS as “1”, as shown in Fig. 5. Therefore, the practical power consumption measurement of 2[#] RIS is consistent with the proposed model in (2). According to the measurement results, the key parameters of 2[#] RIS in the model are: $P_{\text{static}} = 6.52$ W, $P_{i,v}(1, 0) = 0$, and $P_{i,v}(1, 1) = P_{\text{PIN}} = 11.99$ mW, $1 \leq i \leq 512$.

3) 3[#] RIS: The third PIN-diode-based RIS utilized for measurement is a 2-bit coding phase-programmable metasurface [9]-[10], as shown in Fig. 6, which is applied to verify the relationship between the dynamic power consumption and bit resolution of RIS unit cell. The 2-bit digital metasurface operates at frequency $f = 9.5$ GHz with 8×8 programmable elements, and unit cell consists of a hexagonal metal patch and two biasing lines printed on a grounded dielectric substrate. Two PIN diodes are loaded into each RIS unit cell to control the reflection phase. The size of the RIS unit cell is 14 mm \times 14 mm. It is worth mentioning that in the process of this measurement, the ground wire path must be large enough to avoid the nonlinearity caused by the partial voltage of the earth wire resistance.

Firstly, the column of RIS is enabled, respectively. And four coding status (“11”, “10”, “01”, “00”) are set respectively for each column. When provided 1.2 V voltage, the current of each column are shown in the Table II, illustrating that the dynamic power consumption is related to the coding status. Moreover, the current of column cumulation are shown in Table III as well. According to Table II and III, we find that there is a linear relationship between the dynamic power consumption and the number of enabled bits of RIS. Therefore, the practical power consumption measurement of 3[#] RIS is consistent with the proposed model in (2). According to the measurement results, the key parameters of 3[#] RIS in the model are: $P_{i,v}(2, 0) = 0$, and $P_{i,v}(2, 2) = 2P_{i,v}(2, 1) = 2P_{\text{PIN}} = 2.49$ mW, $P_{\text{PIN}} = 1.245$ mW.

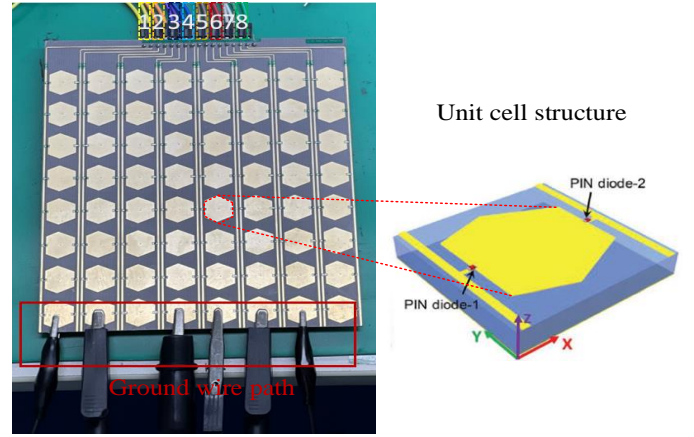


Fig. 6: Photograph of the 3[#] 2-bit RIS.

B. Varactor-diode-based RIS

The fabricated RIS utilized for another verification belongs to the family of varactor-diode-based programmable metasurfaces [11], as shown in Fig. 7(a). It is a 3-bit RIS with 8 coding states and its operating frequency is $f = 3.2$ GHz. The total length and width of this RIS are 0.435 m \times 0.203 m, and the RIS is composed of $N = 8$ columns of unit cells, with $M = 16$ unit cells in each column. Each unit cell has a length and width of 27.2 mm \times 25.4 mm, consisting of the metal patches and varactor diode. The varactor diode is utilized to bridge the metal patches and operated as an adjustable device for controlling the phase shift of EM waves at a particular frequency range.

This RIS can be controlled by column. Our measurement setup and 8 coding states corresponding to the bias voltages applied on the varactors are illustrated in Fig. 7(b). Firstly, 8 reverse bias voltages of 0 V, -3 V, \dots , -8 V, -20 V are applied to the each column of RIS, respectively. As we expected, according to our proposed model, the current in the varactor diodes of the unit cells is negligible. Next, the RIS is enabled from single column to all columns, also applying 8 bias voltages, respectively. The current output is also negligible. It is because that the junction capacitance changes with the bias voltage only when the reverse bias voltage is applied to the varactor, then the phase modulation function can be realized. The reverse bias voltage will thicken the PN junction inside the varactor and prevent the current from passing through, thus the varactor is always in the “off” state when it works. Therefore, the power consumption of varactor-diode-based RISs is $P_{\text{dynamic}} \approx 0$.

The control circuit of 4[#] RIS mainly consists of DAC and operational amplifier, and the static power consumption is measured as $P_{\text{static}} = 0.72$ W for generating 4 control signals. Since $P_{\text{dynamic}} \approx 0$, varactor-diode-based RIS has potential of achieving low power consumption compared with PIN-diode-based RIS. However, it should be noted that the control circuit of varactor-diode based RIS is often much more complicated, i.e., a varactor diode interfaced with voltage level shifter circuitry or DACs, whereas PIN-diode based RIS only needs shift register and FPGA [12]. In addition, most of RISs working in high frequency (i.e., mmWave band) belong to the

TABLE II: Power consumption of each column (Operating voltage = 1.2 V)

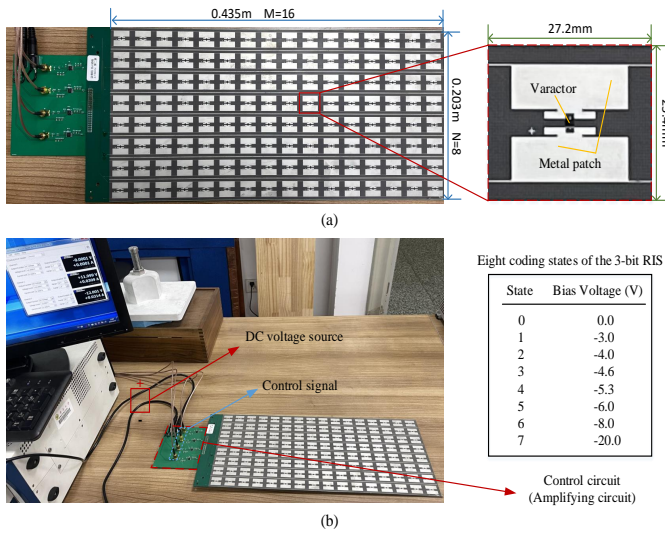
Coding status	The number of column								
	1	2	3	4	5	6	7	8	
"11"	19.0 mW	19.1 mW	19.8 mW	19.8 mW	19.7 mW	19.4 mW	20.0 mW	19.6 mW	
"10"	9.5 mW	9.5 mW	9.5 mW	9.5 mW	9.5 mW	9.7 mW	9.7 mW	9.5 mW	
"01"	9.5 mW	9.6 mW	9.5 mW	10.0 mW	9.5 mW	9.7 mW	10.0 mW	9.7 mW	
"00"	0 mW	0 mW	0 mW	0 mW	0 mW	0 mW	0 mW	0 mW	

TABLE III: Power consumption of column cumulation (Operating voltage = 1.2 V, Coding status = "11")

Cumulative number of columns	1+2	1+3	1+2+3	2+3+4	1+2+3+4	2+3+4+5	1+2+4+5+7	2+4+5+7+8
Measured value	38.4 mW	39.1 mW	57.5 mW	58.2 mW	77.4 mW	77.9 mW	97.2 mW	97.6 mW
Theoretical value	38.0 mW	39.1 mW	57.8 mW	58.7 mW	77.6 mW	78.4 mW	97.7 mW	98.2 mW

TABLE IV: Power consumption of various RISs

RIS	Realization method	Polarization mode	Frequency	Bit resolution	P_{static}	P_{PIN}
1# RIS	PIN diode	Double Polarization	35 GHz	1 bit	15.73 W	12.6 mW
2# RIS	PIN diode	Single Polarization	2.6 GHz	1 bit	6.52 W	12.0 mW
3# RIS	PIN diode	Single Polarization	9.5 GHz	2 bit	/	1.2 mW
4# RIS	Varactor diode	Single Polarization	3.2 GHz	3 bit	0.754 W	0 mW

Fig. 7: Photographs of the 4[#] varactor-diode-based RIS and 8 coding states of the 3-bit RIS.

family of PIN-diode based RIS, because there still remains challenges for designing and manufacturing the varactor-diode based RIS in high frequency band.

The power consumption of various RISs is summarized in Table IV, and the P_{static} and P_{PIN} are supported by practical experiments. Overall, the low power consumption design of RIS is an open research area for further investigation.

IV. CONCLUSION

In this letter, we have carried out the power consumption modeling and experimental validation for RISs. According to the measurement results, it can be summarized that RISs exist static power consumption and dynamic power consumption. The varactor-diode based RIS's dynamic power consumption is almost negligible and the PIN-diode based RIS's dynamic power consumption is related to the polarization mode, controllable bit resolution, working status of RIS, and their quantitative relationship is given in a concise formula which is verified by practical measurements. Practical static power

consumption is measured in our work, shown as a specific constant value for each fabricated RIS, and its accurate model needs further study in future works.

REFERENCES

- [1] T. J. Cui, M. Q. Qi, X. Wan, J. Zhao, and Q. Cheng, "Coding metamaterials, digital metamaterials and programmable metamaterials," *Light Sci. Appl.*, vol. 3, no. 10, pp. e218–e218, 2014.
- [2] Y. Han, W. Tang, S. Jin, C.-K. Wen, and X. Ma, "Large intelligent surface-assisted wireless communication exploiting statistical CSI," *IEEE Trans. Veh. Technol.*, vol. 68, no. 8, pp. 8238–8242, 2019.
- [3] Q. Wu and R. Zhang, "Intelligent reflecting surface enhanced wireless network via joint active and passive beamforming," *IEEE Trans. Wireless Commun.*, vol. 18, no. 11, pp. 5394–5409, 2019.
- [4] C. Huang, A. Zappone, G. C. Alexandropoulos, M. Debbah, and C. Yuen, "Reconfigurable intelligent surfaces for energy efficiency in wireless communication," *IEEE Trans. Wireless Commun.*, vol. 18, no. 8, pp. 4157–4170, 2019.
- [5] L. N. Ribeiro, S. Schwarz, M. Rupp, and A. L. de Almeida, "Energy efficiency of mmwave massive mimo precoding with low-resolution dacs," *IEEE J. Sel. Top. Signal Process.*, vol. 12, no. 2, pp. 298–312, 2018.
- [6] A. Zappone, M. Di Renzo, F. Shams, X. Qian, and M. Debbah, "Overhead-aware design of reconfigurable intelligent surfaces in smart radio environments," *IEEE Trans. Wireless Commun.*, vol. 20, no. 1, pp. 126–141, 2020.
- [7] W. Tang, M. Z. Chen, X. Chen, J. Y. Dai, Y. Han, M. Di Renzo, Y. Zeng, S. Jin, Q. Cheng, and T. J. Cui, "Wireless communications with reconfigurable intelligent surface: Path loss modeling and experimental measurement," *IEEE Trans. Wireless Commun.*, vol. 20, no. 1, pp. 421–439, 2020.
- [8] X. Pei, H. Yin, L. Tan, L. Cao, Z. Li, K. Wang, K. Zhang, and E. Bjornson, "Ris-aided wireless communications: Prototyping, adaptive beamforming, and indoor/outdoor field trials," *IEEE Trans. Wireless Commun.*, vol. 69, no. 12, pp. 8627–8640, 2021.
- [9] L. Zhang, M. Z. Chen, W. Tang, J. Y. Dai, L. Miao, X. Y. Zhou, S. Jin, Q. Cheng, and T. J. Cui, "A wireless communication scheme based on space-and frequency-division multiplexing using digital metasurfaces," *Nat. Electron.*, vol. 4, no. 3, pp. 218–227, 2021.
- [10] L. Zhang, X. Q. Chen, R. W. Shao, J. Y. Dai, Q. Cheng, G. Castaldi, V. Galdi, and T. J. Cui, "Breaking reciprocity with space-time-coding digital metasurfaces," *Adv. Mater.*, vol. 31, no. 41, p. 1904069, 2019.
- [11] J. C. Liang, Q. Cheng, Y. Gao, C. Xiao, S. Gao, L. Zhang, S. Jin, and T. J. Cui, "An angle-insensitive 3-bit reconfigurable intelligent surface," *IEEE Trans. Antennas Propag.*, pp. 1–1, 2021.
- [12] J. Rains, A. Tukmanov, T. J. Cui, L. Zhang, Q. H. Abbasi, M. A. Imran et al., "High-resolution programmable scattering for wireless coverage enhancement: An indoor field trial campaign," *IEEE Trans. Antennas Propag.*, 2022, doi: 10.1109/TAP.2022.3216555.